THE BEST AND BRIGHTEST METAL-POOR STARS

The Astrophysical Journal, 797:13 (11pp), 2014 December 10 doi:10.1088/0004-637X/797/1/13

THE BEST AND BRIGHTEST METAL-POOR STARS*

Kevin C. Schlaufman[1,4,5] and Andrew R. Casey[1,2,3,5]
[1] Kavli Institute for Astrophysics and Space Research, Massachusetts Institute of Technology, Cambridge, MA 02139, USA; kschlauf@mit.edu
[2] Research School of Astronomy and Astrophysics, Australian National University, Canberra, ACT 2611, Australia
[3] Institute of Astronomy, University of Cambridge, Madingley Road, Cambridge CB3 0HA, UK; arc@ast.cam.ac.uk
Received 2014 August 25; accepted 2014 September 15; published 2014 November 19

ABSTRACT

The chemical abundances of large samples of extremely metal-poor (EMP) stars can be used to investigate metal-free stellar populations, supernovae, and nucleosynthesis as well as the formation and galactic chemical evolution of the Milky Way and its progenitor halos. However, current progress on the study of EMP stars is being limited by their faint apparent magnitudes. The acquisition of high signal-to-noise spectra for faint EMP stars requires a major telescope time commitment, making the construction of large samples of EMP star abundances prohibitively expensive. We have developed a new, efficient selection that uses only public, all-sky APASS optical, 2MASS near-infrared, and *WISE* mid-infrared photometry to identify bright metal-poor star candidates through their lack of molecular absorption near 4.6 microns. We have used our selection to identify 11,916 metal-poor star candidates with $V < 14$, increasing the number of publicly available candidates by more than a factor of five in this magnitude range. Their bright apparent magnitudes have greatly eased high-resolution follow-up observations that have identified seven previously unknown stars with [Fe/H] $\lesssim -3.0$. Our follow-up campaign has revealed that $3.8^{+1.3}_{-1.1}$% of our candidates have [Fe/H] $\lesssim -3.0$ and $32.5^{+3.0}_{-2.9}$% have $-3.0 \lesssim$ [Fe/H] $\lesssim -2.0$. The bulge is the most likely location of any existing Galactic Population III stars, and an infrared-only variant of our selection is well suited to the identification of metal-poor stars in the bulge. Indeed, two of our confirmed metal-poor stars with [Fe/H] $\lesssim -2.7$ are within about 2 kpc of the Galactic center. They are among the most metal-poor stars known in the bulge.

Key words: Galaxy: bulge – Galaxy: halo – Galaxy: stellar content – infrared: stars – stars: Population II – stars: statistics

Online-only material: color figures, machine-readable tables

1. INTRODUCTION

The chemical abundances of extremely metal-poor (EMP) stars uniquely illuminate the chemical state of star-forming regions in the progenitor halos of the Milky Way. The relatively low-mass EMP stars still observable today must have formed in star-forming regions seeded with metals by more massive and more primitive stars, perhaps even by metal-free Population III stars. As a result, the chemical abundances of large samples of EMP stars collectively constrain the high-redshift initial mass function, the nucleosynthetic yields and explosive deaths of Population III stars, the production of lithium from Big Bang nucleosynthesis, as well as the galactic chemical evolution of the Milky Way (e.g., Yoshida et al. 2006; Heger & Woosley 2010; Ryan et al. 1999; Cayrel et al. 2004; Beers & Christlieb 2005).

Classical objective prism surveys for metal-poor stars like the HK Survey of Beers et al. (1985, 1992) identified about 1000 candidates with $V \lesssim 14$ based on weak Ca II H and K absorption lines. More recently, the objective prism-based Hamburg/ESO Survey (HES) has identified more than 20,000 candidates using Ca II H and K, but typically with $V \gtrsim 16$ (Wisotzki et al. 1996; Reimers & Wisotzki 1997; Christlieb et al. 2008). Moderate-resolution follow-up observations of candidates from both the HK Survey and HES are still in progress. Taking advantage of the fact that a significant fraction of EMP stars are carbon enhanced, these carbon-enhanced EMP stars (CEMP) stars can also be identified by prominent carbon features in objective-prism data (e.g., Placco et al. 2010, 2011).

The importance of identifying apparently bright metal-poor stars led Frebel et al. (2006b) to perform an independent search of the HES plates for candidates with $9 \lesssim B \lesssim 14$. That search and subsequent moderate-resolution spectroscopy identified about 150 stars with $-3.0 \lesssim$ [Fe/H] $\lesssim -2.0$ and approximately 25 stars with $-4.0 \lesssim$ [Fe/H] $\lesssim -3.0$. The search also led to the discovery of HE 1327-2326, at the time the most iron-poor star known (Frebel et al. 2005; Aoki et al. 2006; Frebel et al. 2006a). High-resolution follow-up observations of this sample are ongoing (e.g., Hollek et al. 2011).

The Sloan Digital Sky Survey (SDSS; York et al. 2000) and the subsequent Sloan Extension for Galactic Understanding and Exploration (SEGUE; Yanny et al. 2009) have also led to the discovery of many EMP stars. Searches based on the weakness of Ca II H and K in SDSS $R \sim 1800$ spectra have confirmed tens of EMP stars with $g \gtrsim 16$, including the star with the lowest-known total metallicity (e.g., Caffau et al. 2011a, 2011b, 2012, 2013; Bonifacio et al. 2012). At the same time, metallicities directly determined from SDSS spectroscopy have led to the confirmation of about 100 EMP stars and the identification of about 1000 very likely EMP stars (e.g., Allende Prieto et al. 2006; Aoki et al. 2013; Norris et al. 2013a). As with objective prism data, prominent carbon features observed in SDSS spectroscopy have led to the confirmation of 24 EMP stars and the identification of about 50 very likely EMP stars with significant carbon enhancements (e.g., Aoki et al. 2008;

* This paper includes data gathered with the 6.5 m Magellan Telescopes located at Las Campanas Observatory, Chile.
[4] Kavli Fellow.
[5] Visiting Astronomer, Kitt Peak National Observatory, National Optical Astronomy Observatory, which is operated by the Association of Universities for Research in Astronomy (AURA) under cooperative agreement with the National Science Foundation.

Lee et al. 2013; Spite et al. 2013). The RAdial Velocity Experiment (RAVE; Steinmetz et al. 2006) was an untargeted spectroscopic survey of bright stars over 20,000 deg^2 of the southern sky that has also identified more than 1000 stars with [Fe/H] $\lesssim -2.0$ (e.g., Fulbright et al. 2010; Kordopatis et al. 2013)

The 1.3 m SkyMapper Telescope at Siding Spring Observatory is poised to produce a flood of new EMP star candidates. The combination of its *ugriz* filter set with a *v* intermediate-band filter covering the spectrum from 367 nm to 398 nm is optimized to identify metal-poor stars (Keller et al. 2007). The SkyMapper-EMP star program is expected to identify a further ~5000 candidates with $9 < g < 15$ and another ~26,000 candidates with $15 < g < 17$. Already, SkyMapper has discovered the most iron-poor star known: SMSS J031300.36−670839.3 (Keller et al. 2014). The chemical abundance pattern of SMSS J031300.36−670839.3 suggests that it likely formed from material enriched by a only a single supernova, indicating that it is the closest link to Population III stars yet found.

Even with tens of thousands of metal-poor star candidates known, their faint apparent magnitudes leave their enormous scientific potential tantalizingly close yet just out of reach. High-resolution spectroscopy (e.g., $R \gtrsim 25{,}000$) with high signal-to-noise (e.g., S/N ~ 100 pixel^{-1} at 400 nm) is critical to fully understand and exploit the chemical abundances of EMP stars. Yet to achieve such spectroscopy takes a prohibitively large amount of 6–10 m class telescope time. For example, the acquisition of a $R \sim 25{,}000$ spectrum with S/N ~ 100 pixel^{-1} at 400 nm for an EMP star with $V \approx 16$ takes about four hours using the MIKE spectrograph on the Magellan Clay Telescope. The same resolution and S/N could be achieved for a $V \approx 13$ EMP star in only 15 minutes. The lack of apparently bright metal-poor stars has restricted the most comprehensive metal-poor star abundance analyses yet published to only a few hundred objects (Norris et al. 2013a, 2013b; Yong et al. 2013a, 2013b; Roederer et al. 2014).

To help identify large samples of apparently bright EMP stars, we have developed a new, efficient metal-poor star candidate selection that uses only public, all-sky APASS optical, 2MASS near-infrared, and *WISE* mid-infrared photometry. Metal-rich stars are bright in the 2MASS *J* and *WISE* *W*1 bands, but faint in the *WISE* *W*2 band due to molecular absorption. Metal-poor stars are bright in all three bands. We specify our sample selection in Section 2. We detail our observational follow up, stellar parameter derivation, and carbon abundance analysis in Section 3. We discuss our results and their implications in Section 4, and we summarize our findings in Section 5.

2. SAMPLE SELECTION

As input to our sample selection, we use the APASS DR6 Catalog, the 2MASS All-Sky Point Source Catalog, and the AllWISE Source Catalog (Henden et al. 2012; Skrutskie et al. 2006; Wright et al. 2010; Mainzer et al. 2011). We describe the data quality cuts we apply in the Appendix.

We show the physical basis for our selection in Figure 1. Strong molecular absorption is present in the atmospheres of stars with effective temperature $T_{\rm eff}$ in the range $4500\,{\rm K} \lesssim T_{\rm eff} \lesssim 5500$ K for all surface gravities $\log g$, strongly affecting fluxes in the *WISE* *W*2 band at 4.6 microns. While this strong absorption persists down to [Fe/H] ~ −2.0 in cool stars, it disappears at higher metallicity for hotter stars. As a result, we use 2MASS $J-H$ color as a reddening-insensitive proxy for effective temperature and select stars with $0.45 \leqslant J-H \leqslant 0.6$. We also eliminate nearly all solar neighborhood interlopers by selecting objects with $W3 > 8$.

To make the qualitative observation that *W*2 flux can be used to identify metal-poor stars more quantitative, we download all stars from SIMBAD with published stellar parameters in the range $3000\,{\rm K} < T_{\rm eff} < 8000$ K and cross-match the result with the 2MASS All-Sky Point Source and AllWISE Source catalogs using TOPCAT[6] (Taylor 2005). *WISE* photometry is in Vega magnitudes, so a star with a spectral energy distribution (SED) similar to Vega will have all colors composed of *WISE* filters equal to zero. Vega is a hot star with no molecular absorption in *W*2, so metal-poor stars with no molecular absorption in *W*2 should have similar SEDs to Vega and have $W1 - W2 \approx 0$. More metal-rich stars will have slightly bluer $W1 - W2$ colors, so we require $-0.04 \leqslant W1 - W2 \leqslant 0.04$. Empirically, we find that selecting stars with $J - W2 > 0.5$ has a small positive impact on the yield of metal-poor stars by removing a significant number of solar metallicity contaminants.

We used this pure color selection for our initial target catalog, then used the metal-poor stars identified on each observing run to optimize the selection in three more ways. First, we used the metal-poor stars we identified to train a logistic regression model[7] to predict the probability that a star that passes our color cuts is metal-poor based on its $J-H$, $J-K$, $J-W1$, and $J-W2$ colors. Second, we noted that the metal-poor stars we discovered had red $J-W2$ colors at constant $B-V$. Third, we noted that none of our metal-poor stars had very red $B-V$ colors, so we require $B-V < 1.2$. In summary, our final list of selection criteria is:

1. $0.45 \leqslant J-H \leqslant 0.6$
2. $W3 > 8$
3. $-0.04 \leqslant W1-W2 \leqslant 0.04$
4. $J-W2 > 0.5$
5. $e^z/(1+e^z) > 0.13$, where $z = -2.534642 + 16.241145(J-H) - 9.271496(J-K) - 40.009841(J-W1) + 38.514156(J-W2)$
6. $J-W2 > 0.5\,[(B-V)-0.8]+0.6$
7. $B-V < 1.2$

We estimate our completeness by calculating the fraction of stars in the compilation of Yong et al. (2013a) that we would recover with our selection. Of the 29 stars from Yong et al. (2013a) that pass our *WISE* data quality checks and are in the range $0.45 \leqslant J-H \leqslant 0.6$, criteria (1)–(5) identify 18 (62%) as metal-poor candidates with infrared photometry alone. Of the 16 stars that pass criteria (1)–(5) and that have APASS data, 14 (88%) are identified as metal-poor by our full selection. We also confirm that our selection correctly identifies SMSS J031300.36−670839.3 as a metal-poor candidate. After applying criteria (1)–(5), we are left with 22,721 metal-poor star candidates with $V < 14$. Applying our full selection leaves us with 11,916 metal-poor star candidates with $V < 14$.

We subsequently found that most of our false positives are stars with emission in the cores of the Ca II H and K lines as well as broad absorption lines demonstrating significant projected rotation velocities. These objects are likely young stars, as stars in the range of $J-H$ we explore spin-down to slower rotation velocities within ≈650 Myr (Irwin & Bouvier 2009). Since our selection is based on an excess of *W*2 flux relative to that expected for solar-metallicity stars, these stars are selected

[6] http://www.star.bristol.ac.uk/~mbt/topcat/

[7] See Section 3.1 of Schlaufman (2014) for a detailed discussion of logistic regression.

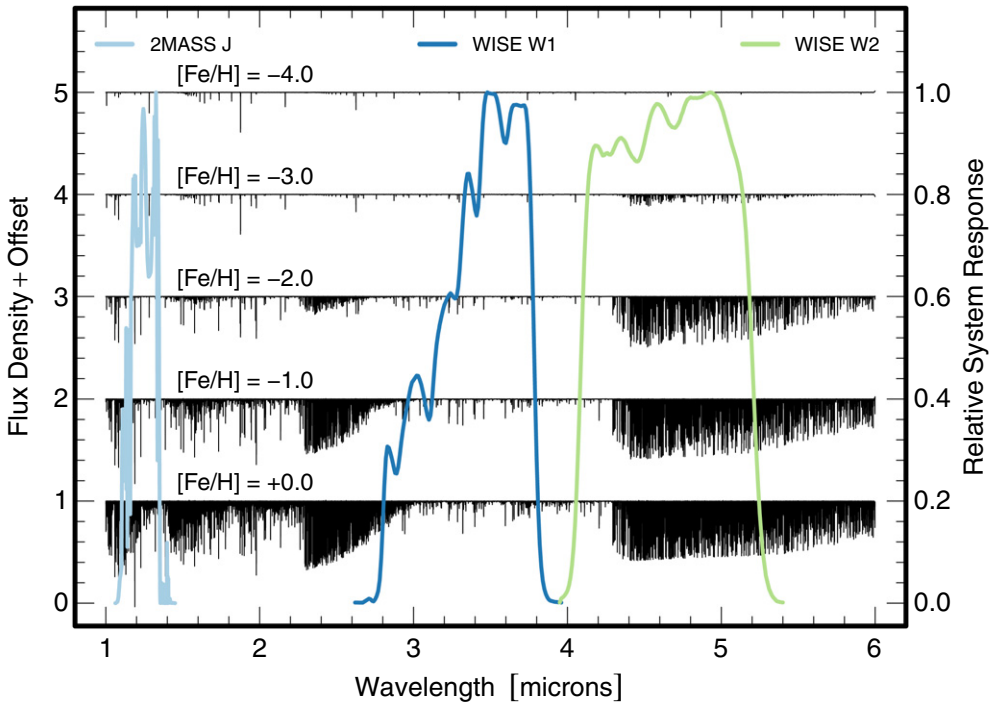

Figure 1. Brott & Hauschildt (2005) theoretical spectra for stellar atmospheres with the metallicity given in the plot, assuming $[\alpha/\mathrm{Fe}] = +0.4$ for $[\mathrm{Fe/H}] \leqslant -1$. We assume $T_{\mathrm{eff}} = 4800$ K – the median of our sample – and $\log g = 1.5$, though the features are insensitive to $\log g$. The light blue curve is the relative system response curve (RSR) for the 2MASS J band (1.2μ), the dark blue curve is the RSR for the *WISE* $W1$ band (3.4μ), and the green curve is the RSR for the *WISE* $W2$ band (4.6μ). Strong molecular absorption is present in $W2$ down to $[\mathrm{Fe/H}] = -2$, implying that colors involving $W2$ can help select metal-poor stars from photometry alone.

(A color version of this figure is available in the online journal.)

because they are orbited by hot debris disks. The occurrence of debris declines sharply with age for stars in this range of color, so hot debris is another signal of youth (e.g., Plavchan et al. 2005; Rhee et al. 2007). For all of these reasons, our selection would also be very useful to select young stars in the field. The addition of soft X-ray data to our selection from the upcoming all-sky X-ray survey by the eROSITA satellite will likely enable a clean separation of metal-poor stars and young stars (Merloni et al. 2012).

3. OBSERVATIONAL FOLLOW-UP AND DETERMINATION OF STELLAR PARAMETERS

We followed up our metal-poor star candidates with the Mayall 4 m/Echelle,[8] Gemini South/GMOS-S (Hook et al. 2004),[9] and Magellan/MIKE (Bernstein et al. 2003) telescopes and spectrographs. We observed 98 stars with the Mayall 4 m/Echelle on 2013 June 25–27, using the 58.5–63 grating, cross-disperser 226–2, 1.″0 slit, order 2, and the blue camera, corrector, and collimator. While we found no EMP stars on our Mayall 4 m/Echelle run, we did use the data to significantly improve our selection. We do not consider it further. We observed 90 stars with Gemini South/GMOS-S in service mode from 2014 March to July. We used the long-slit mode with the B1200 grating, 0.″5 slit, and central wavelength 450 nm, yielding resolution $R \approx 3700$ spectra between 380 nm and 520 nm. We observed 416 stars with Magellan/MIKE on 2014 June 21–23 and July 8–10. We used the 0.″7 slit and the standard blue and red grating azimuths, yielding spectra between 335 nm and 950 nm with resolution $R \approx 41{,}000$ in the blue and $R \approx 35{,}000$ in the red.

[8] Program 2013A-0186.

[9] Programs GS-2014A-Q-8 and GS-2014A-Q-74.

3.1. Gemini South/GMOS-S Data

We derive stellar parameters for the stars we observed with Gemini South/GMOS-S by comparing the observed spectra with model spectra in a Markov Chain Monte Carlo (MCMC) framework. Our code creates model spectra by interpolating from the high-resolution AMBRE synthetic library (de Laverny et al. 2012) for each sampling of T_{eff}, $\log g$, [Fe/H], and mean α-element enhancement $[\alpha/\mathrm{Fe}]$. Additional phenomena that transform the observed spectra were included as free parameters: radial velocity, continuum coefficients, broadening, and outlier pixels. There are 11 total model parameters: T_{eff}, $\log g$, [Fe/H], $[\alpha/\mathrm{Fe}]$, redshift z, continuum coefficients $\{c_i\}_{i=1}^{3}$, logarithm of fractionally underestimated variance $\log f$, outlier fraction P_o, and additive outlier variance V_o.

We numerically optimized the model parameters before performing the MCMC analysis using `emcee`[10] (Foreman-Mackey et al. 2013). We took the starting point for 200 walkers as a multi-dimensional ball around the optimized point. We allowed for 10^6 total steps for the burn-in phase, and we used a further 2×10^5 steps to sample the posterior. The auto-correlation times, mean acceptance fractions, and values of the model parameters with each step suggest that the analyses are converged by at most 3×10^5 steps. We give the mean of the posterior and credible intervals for stellar parameters and radial velocity in Table 1.

3.2. Magellan/MIKE Data

We derive stellar parameters for the stars we observed with Magellan/MIKE by classical methods. Individual echelle orders were normalized with a spline function before stitching them

[10] http://dan.iel.fm/emcee/current/

Table 1
Metal-poor Candidate Velocities and Stellar Parameters for Stars Observed with Gemini South/GMOS-S

Object (2MASS)	$v_{\rm los}$ (km s^{-1})	$T_{\rm eff}$ (K)	log g	[Fe/H]	[α/Fe]
J121325.53-380021.6	$25.8^{5.2}_{-2.3}$	5339^{+64}_{-69}	$4.64^{+0.12}_{-0.11}$	$-0.47^{+0.07}_{-0.07}$	$0.24^{+0.04}_{-0.04}$
J121812.33-372106.5	$-26.3^{+27.8}_{-0.1}$	3499^{+41}_{-27}	$4.56^{+0.40}_{-0.16}$	$0.77^{+0.18}_{-0.72}$	$0.21^{+0.03}_{-0.01}$
J122934.47-323307.4	$231.2^{+0.2}_{-0.2}$	5002^{+9}_{-7}	$2.33^{+0.03}_{-0.03}$	$-1.42^{+0.01}_{-0.01}$	$0.44^{+0.02}_{-0.02}$
J135216.59-355425.8	$150.0^{+0.3}_{-0.3}$	5208^{+15}_{-17}	$3.01^{+0.04}_{-0.04}$	$-1.62^{+0.02}_{-0.03}$	$0.45^{+0.02}_{-0.03}$
J135841.47-315110.2	$5.6^{+0.3}_{-0.3}$	5256^{+17}_{-14}	$4.80^{+0.03}_{-0.03}$	$-0.26^{+0.02}_{-0.02}$	$0.15^{+0.01}_{-0.01}$
J141733.51-274514.4	$35.2^{+0.4}_{-0.4}$	4874^{+21}_{-20}	$3.81^{+0.05}_{-0.05}$	$-0.24^{+0.02}_{-0.01}$	$0.12^{+0.02}_{-0.02}$
J141924.83-230737.1	$39.3^{+0.3}_{-0.3}$	4766^{+24}_{-16}	$4.48^{+0.08}_{-0.05}$	$-0.55^{+0.03}_{-0.03}$	$0.06^{+0.01}_{-0.01}$
J150159.91-261349.4	$-107.3^{+1.2}_{-1.3}$	4969^{+44}_{-49}	$2.35^{+0.16}_{-0.13}$	$-1.02^{+0.04}_{-0.07}$	$0.41^{+0.05}_{-0.05}$
J150237.42-244219.1	$-97.1^{+1.2}_{-1.1}$	5182^{+59}_{-64}	$3.68^{+0.13}_{-0.10}$	$-0.45^{+0.04}_{-0.05}$	$0.21^{+0.03}_{-0.02}$
J150601.36-250831.9	$5.4^{+0.8}_{-1.0}$	4969^{+25}_{-20}	$4.27^{+0.08}_{-0.06}$	$-0.18^{+0.05}_{-0.05}$	$0.05^{+0.02}_{-0.03}$
J150652.36-254707.1	$-55.9^{+1.1}_{-0.9}$	4678^{+31}_{-28}	$4.34^{+0.08}_{-0.08}$	$-0.50^{+0.06}_{-0.06}$	$0.05^{+0.03}_{-0.03}$
J150943.10-202529.9	$-24.5^{+1.0}_{-1.1}$	5002^{+33}_{-33}	$4.63^{+0.09}_{-0.06}$	$-0.33^{+0.05}_{-0.09}$	$0.07^{+0.02}_{-0.02}$
J154825.93-395925.8	$7.8^{+0.7}_{-0.7}$	5862^{+34}_{-35}	$4.13^{+0.07}_{-0.07}$	$-0.35^{+0.04}_{-0.05}$	$0.18^{+0.04}_{-0.05}$
J155145.68-393538.2	$-24.9^{+1.6}_{-1.7}$	5469^{+58}_{-45}	$3.62^{+0.13}_{-0.14}$	$-0.28^{+0.04}_{-0.05}$	$0.26^{+0.04}_{-0.05}$
J155212.12-393422.7	$-41.0^{+0.6}_{-0.6}$	6075^{+38}_{-35}	$4.49^{+0.13}_{-0.12}$	$-0.07^{+0.04}_{-0.05}$	$0.19^{+0.04}_{-0.06}$
J155410.62-325516.7	$156.1^{+0.3}_{-0.3}$	5069^{+17}_{-16}	$2.54^{+0.04}_{-0.03}$	$-1.27^{+0.02}_{-0.02}$	$0.39^{+0.00}_{-0.01}$
J155422.58-334156.7	$-18.9^{+0.3}_{-0.4}$	5636^{+32}_{-30}	$4.12^{+0.04}_{-0.04}$	$-0.11^{+0.04}_{-0.03}$	$0.15^{+0.01}_{-0.02}$
J155730.10-293922.7	$119.8^{+0.1}_{-7.2}$	5108^{+47}_{-23}	$2.00^{+0.40}_{-0.36}$	$-2.77^{+0.11}_{-0.05}$	$0.31^{+0.13}_{-0.06}$
J155837.56-373411.3	$-32.3^{+0.3}_{-0.3}$	6568^{+10}_{-11}	$4.56^{+0.03}_{-0.02}$	$-0.41^{+0.01}_{-0.01}$	$0.11^{+0.02}_{-0.02}$
J155848.49-360337.0	$25.8^{+0.3}_{-0.3}$	5348^{+23}_{-28}	$4.76^{+0.04}_{-0.05}$	$-0.39^{+0.02}_{-0.03}$	$0.16^{+0.01}_{-0.01}$
J155921.32-341626.1	$-19.4^{+0.3}_{-0.4}$	5966^{+18}_{-29}	$4.55^{+0.04}_{-0.05}$	$-0.03^{+0.02}_{-0.02}$	$0.10^{+0.02}_{-0.02}$
J155922.28-385356.0	$-23.5^{+0.3}_{-0.3}$	5139^{+21}_{-22}	$3.76^{+0.04}_{-0.05}$	$-0.46^{+0.02}_{-0.02}$	$0.24^{+0.01}_{-0.01}$
J155952.35-320738.8	$75.3^{+0.5}_{-0.5}$	5225^{+19}_{-17}	$4.34^{+0.04}_{-0.04}$	$-0.91^{+0.03}_{-0.03}$	$0.43^{+0.02}_{-0.02}$
J160058.80-330756.4	$31.9^{+0.4}_{-0.4}$	5826^{+18}_{-16}	$4.36^{+0.03}_{-0.03}$	$-0.00^{+0.03}_{-0.01}$	$0.10^{+0.02}_{-0.02}$
J160529.44-254335.1	$-43.9^{+0.4}_{-0.4}$	4213^{+11}_{-10}	$3.74^{+0.08}_{-0.05}$	$-0.96^{+0.03}_{-0.03}$	$-0.09^{+0.01}_{-0.01}$
J160604.52-350819.5	$24.9^{+0.3}_{-0.3}$	5147^{+18}_{-16}	$4.77^{+0.03}_{-0.03}$	$-0.31^{+0.02}_{-0.02}$	$0.13^{+0.01}_{-0.01}$
J160611.18-362035.6	$-48.7^{+0.4}_{-0.4}$	5347^{+23}_{-22}	$3.90^{+0.05}_{-0.04}$	$-0.40^{+0.02}_{-0.02}$	$0.20^{+0.02}_{-0.02}$
J160616.44-323710.3	$-22.0^{+1.2}_{-1.1}$	5696^{+45}_{-37}	$4.03^{+0.10}_{-0.08}$	$-0.41^{+0.04}_{-0.04}$	$0.14^{+0.04}_{-0.04}$
J160645.42-321617.9	$-18.2^{+0.6}_{-0.6}$	5946^{+28}_{-27}	$4.34^{+0.06}_{-0.06}$	$-0.24^{+0.02}_{-0.02}$	$0.16^{+0.03}_{-0.04}$
J160656.06-370731.4	$11.9^{+0.5}_{-0.5}$	6595^{+15}_{-15}	$4.33^{+0.05}_{-0.04}$	$-0.34^{+0.02}_{-0.02}$	$0.15^{+0.03}_{-0.03}$
J160732.39-225038.1	$-41.6^{+0.4}_{-0.4}$	6185^{+40}_{-19}	$4.56^{+0.38}_{-0.04}$	$-0.31^{+0.02}_{-0.20}$	$0.03^{+0.02}_{-0.34}$
J160735.32-320847.2	$31.6^{4.2}_{-15.9}$	4969^{+43}_{-92}	$3.88^{+0.88}_{-0.08}$	$-0.37^{+0.07}_{-1.80}$	$0.10^{+0.04}_{-0.24}$
J160741.38-331457.5	$-44.8^{+0.3}_{-0.4}$	5780^{+15}_{-17}	$4.18^{+0.03}_{-0.03}$	$-0.46^{+0.02}_{-0.02}$	$0.26^{+0.02}_{-0.02}$
J160808.90-294321.0	$0.4^{+0.4}_{-0.4}$	5633^{18}_{-18}	$4.14^{+0.04}_{-0.03}$	$-0.25^{+0.01}_{-0.02}$	$0.14^{+0.02}_{-0.02}$
J160813.89-201718.1	$-76.0^{+1.3}_{-1.4}$	5695^{+47}_{-39}	$4.38^{+0.08}_{-0.06}$	$-0.18^{+0.04}_{-0.03}$	$0.12^{+0.03}_{-0.04}$
J160842.93-282018.2	$46.4^{+1.2}_{-1.0}$	5508^{+27}_{-23}	$4.50^{+0.05}_{-0.04}$	$-0.43^{+0.05}_{-0.04}$	$0.12^{+0.03}_{-0.04}$
J161011.26-344622.6	$-2.5^{+0.5}_{-0.5}$	5468^{+27}_{-25}	$4.65^{+0.06}_{-0.04}$	$-0.26^{+0.02}_{-0.03}$	$0.06^{+0.02}_{-0.02}$
J161039.68-244356.5	$35.2^{+0.4}_{-0.4}$	4988^{+37}_{-24}	$3.18^{+0.06}_{-0.05}$	$-0.65^{+0.03}_{-0.03}$	$0.32^{+0.02}_{-0.02}$
J161058.76-281143.5	$114.4^{+0.3}_{-1.1}$	5215^{+45}_{-72}	$2.78^{+0.11}_{-0.41}$	$-0.69^{+0.05}_{-0.06}$	$0.32^{+0.18}_{-0.03}$
J161114.94-320449.4	$-41.4^{+0.3}_{-0.3}$	5389^{+19}_{-18}	$3.88^{+0.04}_{-0.04}$	$-0.46^{+0.02}_{-0.02}$	$0.20^{+0.01}_{-0.02}$
J161146.67-242705.5	$-4.9^{+2.1}_{-1.6}$	5578^{+55}_{-52}	$4.16^{+0.12}_{-0.11}$	$-0.39^{+0.09}_{-0.06}$	$0.17^{+0.07}_{-0.05}$
J161211.01-281812.7	$-3.4^{+1.1}_{-0.8}$	5905^{+30}_{-34}	$4.80^{+0.05}_{-0.05}$	$-0.17^{+0.03}_{-0.03}$	$-0.06^{+0.03}_{-0.02}$
J161328.28-201340.6	$-76.0^{+0.6}_{-0.7}$	6119^{+30}_{-32}	$4.46^{+0.11}_{-0.07}$	$-0.13^{+0.04}_{-0.04}$	$0.17^{+0.04}_{-0.03}$
J161343.74-251738.5	$11.6^{+0.4}_{-0.4}$	6062^{+16}_{-15}	$4.23^{+0.03}_{-0.03}$	$-0.23^{+0.02}_{-0.02}$	$0.12^{+0.02}_{-0.01}$
J161357.00-275710.1	$1.7^{+1.2}_{-1.1}$	5749^{+47}_{-20}	$4.69^{+0.07}_{-0.06}$	$-0.27^{+0.03}_{-0.03}$	$0.02^{+0.04}_{-0.04}$
J161411.20-203338.2	$-118.4^{+1.7}_{-1.8}$	6112^{+44}_{-52}	$4.10^{+0.16}_{-0.13}$	$-0.22^{+0.04}_{-0.04}$	$0.23^{+0.10}_{-0.09}$
J161501.58-233935.6	$-0.1^{+1.1}_{-1.0}$	4994^{+68}_{-90}	$3.79^{+0.09}_{-0.20}$	$-0.51^{+0.10}_{-0.05}$	$0.15^{+0.03}_{-0.04}$
J161548.06-235537.7	$-60.3^{+0.6}_{-0.6}$	6059^{+26}_{-24}	$4.09^{+0.07}_{-0.06}$	$-0.26^{+0.02}_{-0.03}$	$0.12^{+0.03}_{-0.04}$
J161642.05-325700.1	$-159.5^{+0.5}_{-0.5}$	5420^{+24}_{-23}	$3.58^{+0.05}_{-0.05}$	$-1.52^{+0.03}_{-0.04}$	$0.41^{+0.03}_{-0.03}$
J161652.02-215423.7	$70.0^{+0.5}_{-0.5}$	4771^{+23}_{-16}	$3.80^{+0.06}_{-0.04}$	$-0.22^{+0.05}_{-0.04}$	$0.02^{+0.02}_{-0.02}$
J161751.67-334450.6	$-16.9^{+0.4}_{-0.4}$	5926^{+25}_{-21}	$4.60^{+0.04}_{-0.03}$	$-0.19^{+0.02}_{-0.03}$	$0.12^{+0.02}_{-0.02}$
J161755.06-250116.5	$124.6^{+1.9}_{-0.9}$	6216^{+88}_{-73}	$3.63^{+0.41}_{-0.45}$	$-0.42^{+0.13}_{-0.25}$	$0.22^{+0.27}_{-0.26}$
J162034.43-205657.8	$42.1^{+1.3}_{-1.0}$	5314^{+40}_{-35}	$4.18^{+0.08}_{-0.07}$	$-0.28^{+0.02}_{-0.03}$	$0.14^{+0.03}_{-0.03}$

Table 1
(Continued)

Object (2MASS)	$v_{\rm los}$ (km s^{-1})	$T_{\rm eff}$ (K)	log g	[Fe/H]	[α/Fe]
J162047.14-260616.3	$-88.0^{+1.5}_{-1.7}$	5649^{+60}_{-43}	$3.68^{+0.19}_{-0.12}$	$0.23^{+0.05}_{-0.06}$	$0.25^{+0.05}_{-0.06}$
J162318.05-311043.1	$-44.4^{+0.9}_{-0.9}$	5124^{+83}_{-62}	$3.92^{+0.19}_{-0.13}$	$-0.54^{+0.07}_{-0.06}$	$0.27^{+0.04}_{-0.05}$
J162353.51-315154.7	$-22.6^{+0.5}_{-0.5}$	4689^{+16}_{-16}	$3.21^{+0.08}_{-0.05}$	$-0.79^{+0.03}_{-0.03}$	$0.10^{+0.02}_{-0.02}$
J162546.95-335412.0	$-25.9^{+0.5}_{-0.5}$	5994^{+32}_{-27}	$4.47^{+0.08}_{-0.07}$	$-0.24^{+0.02}_{-0.02}$	$0.13^{+0.03}_{-0.03}$
J162607.92-202528.0	$1.2^{+0.9}_{-0.9}$	5457^{+61}_{-54}	$4.34^{+0.10}_{-0.09}$	$-0.46^{+0.06}_{-0.04}$	$0.09^{+0.03}_{-0.04}$
J162747.03-331403.1	$-59.1^{+0.5}_{-0.5}$	5265^{+40}_{-72}	$3.64^{+0.07}_{-0.06}$	$-0.15^{+0.04}_{-0.05}$	$0.33^{+0.02}_{-0.02}$
J163026.14-334249.8	$-47.4^{+0.5}_{-0.6}$	6426^{+16}_{-17}	$4.11^{+0.05}_{-0.05}$	$-0.44^{+0.02}_{-0.02}$	$0.18^{+0.03}_{-0.04}$
J163524.07-335950.9	$-29.4^{+0.4}_{-0.4}$	5627^{+19}_{-19}	$4.74^{+0.04}_{-0.03}$	$-0.39^{+0.03}_{-0.03}$	$0.07^{+0.01}_{-0.01}$
J171257.15-221421.5	$-50.9^{+1.4}_{-1.3}$	6120^{+29}_{-33}	$4.33^{+0.16}_{-0.13}$	$-0.31^{+0.03}_{-0.04}$	$0.07^{+0.10}_{-0.10}$
J171305.97-344246.8	$-53.8^{+1.2}_{-1.1}$	6760^{+28}_{-34}	$4.29^{+0.12}_{-0.12}$	$-0.48^{+0.03}_{-0.03}$	$0.27^{+0.06}_{-0.06}$
J171346.40-225227.0	$-43.3^{+0.4}_{-0.4}$	5693^{+50}_{-12}	$3.68^{+0.99}_{-0.03}$	$-0.20^{+0.02}_{-0.33}$	$0.07^{+0.01}_{-0.36}$
J171514.13-225143.6	$-56.2^{+0.4}_{-0.6}$	5940^{+29}_{-19}	$3.87^{+0.09}_{-0.05}$	$-0.16^{+0.02}_{-0.03}$	$0.13^{+0.02}_{-0.05}$
J180856.81-210630.0	$-58.0^{+1.2}_{-1.2}$	6327^{+31}_{-24}	$4.17^{+0.13}_{-0.21}$	$-0.21^{+0.03}_{-0.03}$	$-0.00^{+0.10}_{-0.07}$
J181503.64-375120.7	$-70.9^{+0.8}_{-0.8}$	5106^{+33}_{-30}	$1.86^{+0.27}_{-0.16}$	$-2.59^{+0.06}_{-0.06}$	$0.38^{+0.07}_{-0.08}$
J181919.19-202925.4	$-34.2^{+0.5}_{-0.5}$	6083^{+17}_{-20}	$3.51^{+0.02}_{-0.01}$	$0.07^{+0.02}_{-0.03}$	$0.12^{+0.02}_{-0.03}$
J181931.28-371313.6	$-195.5^{+0.3}_{-0.5}$	5001^{+21}_{-205}	$2.13^{+0.05}_{-1.93}$	$-1.48^{+0.02}_{-0.69}$	$0.43^{+0.03}_{-0.24}$
J182030.65-201601.3	$-21.4^{+1.1}_{-1.1}$	5922^{+50}_{-38}	$4.79^{+0.12}_{-0.06}$	$-0.26^{+0.03}_{-0.03}$	$-0.05^{+0.03}_{-0.06}$
J182049.23-341948.0	$-164.4^{+0.6}_{-0.6}$	5129^{+34}_{-53}	$2.33^{+0.09}_{-0.15}$	$-1.82^{+0.04}_{-0.07}$	$0.44^{+0.05}_{-0.04}$
J182938.67-201048.4	$-111.8^{+1.4}_{-1.3}$	6411^{+25}_{-25}	$4.49^{+0.10}_{-0.08}$	$-0.20^{+0.03}_{-0.03}$	$-0.00^{+0.05}_{-0.06}$
J183214.23-382940.7	$-42.5^{+0.6}_{-0.7}$	5332^{+36}_{-33}	$2.46^{+0.13}_{-0.13}$	$-1.13^{+0.04}_{-0.04}$	$0.55^{+0.04}_{-0.05}$
J183713.28-314109.3	$-223.6^{+0.8}_{-0.9}$	5196^{+30}_{-32}	$1.64^{+0.20}_{-0.28}$	$-2.49^{+0.05}_{-0.07}$	$0.40^{+0.07}_{-0.08}$
J192532.78-282858.1	$-2.0^{+1.0}_{-1.1}$	5104^{+72}_{-65}	$3.83^{+0.17}_{-0.12}$	$-0.98^{+0.07}_{-0.05}$	$0.49^{+0.06}_{-0.06}$
J201524.98-222100.7	$10.0^{+0.4}_{-0.3}$	4649^{+10}_{-11}	$4.42^{+0.03}_{-0.03}$	$-0.66^{+0.03}_{-0.03}$	$0.27^{+0.01}_{-0.01}$
J201940.99-292226.8	$-72.7^{+2.1}_{-2.1}$	5381^{+120}_{-20}	$3.62^{+0.15}_{-0.05}$	$-0.47^{+0.09}_{-0.05}$	$0.16^{+0.03}_{-0.04}$
J202148.39-291746.7	$-8.7^{+0.9}_{-1.0}$	5211^{+44}_{-34}	$4.60^{+0.11}_{-0.06}$	$-0.25^{+0.05}_{-0.05}$	$0.02^{+0.02}_{-0.03}$
J202442.85-261900.3	$8.9^{+1.1}_{-1.1}$	5752^{+21}_{-34}	$4.70^{+0.06}_{-0.06}$	$-0.13^{+0.04}_{-0.05}$	$0.07^{+0.04}_{-0.03}$
J202737.90-262741.7	$-44.1^{+0.2}_{-0.2}$	5204^{+12}_{-11}	$4.05^{+0.02}_{-0.02}$	$-0.58^{+0.02}_{-0.01}$	$0.37^{+0.01}_{-0.01}$
J202845.49-263810.3	$-83.2^{+0.2}_{-0.2}$	5827^{+11}_{-11}	$4.17^{+0.02}_{-0.02}$	$-0.72^{+0.02}_{-0.02}$	$0.37^{+0.02}_{-0.02}$
J202900.62-215735.4	$15.5^{+0.9}_{-0.9}$	5060^{+34}_{-43}	$4.01^{+0.05}_{-0.14}$	$-0.50^{+0.06}_{-0.04}$	$0.32^{+0.04}_{-0.03}$
J203019.13-284439.7	$-59.4^{+1.1}_{-0.9}$	5087^{+32}_{-36}	$4.69^{+0.07}_{-0.07}$	$-0.39^{+0.05}_{-0.04}$	$0.05^{+0.02}_{-0.02}$
J203133.17-305412.5	$42.3^{+1.0}_{-0.8}$	5274^{+62}_{-37}	$4.77^{+0.08}_{-0.07}$	$-0.35^{+0.05}_{-0.05}$	$0.04^{+0.02}_{-0.02}$
J203733.35-364545.3	$-44.4^{+0.4}_{-0.4}$	4333^{+16}_{-14}	$4.38^{+0.07}_{-0.08}$	$-0.82^{+0.02}_{-0.02}$	$0.01^{+0.01}_{-0.02}$
J203757.80-251825.3	$-9.7^{+0.3}_{-0.3}$	5348^{+31}_{-34}	$4.75^{+0.05}_{-0.05}$	$-0.36^{+0.03}_{-0.04}$	$0.16^{+0.01}_{-0.02}$
J203819.45-275047.7	$99.5^{+0.1}_{-7.7}$	5246^{+33}_{-33}	$3.90^{+0.05}_{-0.06}$	$-0.56^{+0.04}_{-0.04}$	$0.21^{+0.02}_{-0.02}$
J204106.23-325135.9	$69.8^{+1.1}_{-0.7}$	5002^{+54}_{-28}	$4.76^{+0.10}_{-0.07}$	$-0.62^{+0.04}_{-0.04}$	$0.36^{+0.02}_{-0.02}$
J204430.69-293653.4	$17.2^{+1.0}_{-1.0}$	4865^{+27}_{-27}	$4.73^{+0.06}_{-0.07}$	$-0.27^{+0.10}_{-0.03}$	$0.04^{+0.02}_{-0.02}$
J204611.88-383311.8	$39.8^{+1.9}_{-1.8}$	5057^{+52}_{-55}	$2.81^{+0.12}_{-0.13}$	$-1.23^{+0.08}_{-0.07}$	$0.29^{+0.09}_{-0.09}$

together, forming a contiguous spectrum from 335–950 nm. Our spectra typically have S/N $\approx$ 50 pixel^{-1} at 550 nm. We determined radial velocities by cross correlation with the rest-frame spectrum of a metal-poor giant, then Doppler shifted the data to the rest frame. We measured equivalent widths of Fe I and II lines by fitting Gaussian profiles using the approach described by Casey (2014). All transition measurements were visually inspected and we discarded poorly fit lines. We sourced our atomic data from Roederer et al. (2010) and our molecular data (CH) from Masseron et al. (2014). We used Castelli & Kurucz (2004) α-enhanced model atmospheres.

We estimated our stellar parameters through excitation and ionization balance. We found $T_{\rm eff}$ by enforcing a zero trend in Fe I abundance with excitation potential. We adjusted log g until the mean Fe I and Fe II abundances matched within 0.005 dex. Similarly, we adjusted the model atmosphere until it matched the mean Fe I abundance. Finally, we found microturbulence ξ by ensuring a zero trend in abundance and reduced equivalent width for all Fe I lines. These four conditions were simultaneously met to derive stellar parameters for the entire Magellan/MIKE sample, which we give in Table 2. Given the spectral resolution and S/N of our sample, the uncertainties in stellar parameters for the Magellan/MIKE sample are conservatively estimated to be of order 100 K in $T_{\rm eff}$, 0.2 in log g, 0.1 in [Fe/H], and 0.1 km s^{-1} in ξ. Some of our candidates proved to be so metal rich that an equivalent width analysis was inappropriate. We do not report stellar parameters for these objects and express the reason in the comment column of Table 2. We give the photometry for our Magellan/MIKE sample in Table 3. We selected our targets from our larger catalog because their

Table 2
Metal-poor Candidate Velocities and Stellar Parameters for Stars Observed with Magellan/MIKE

Object (2MASS)	v_{los} (km s^{-1})	T_{eff} (K)	log g	[Fe/H]	ξ (km s^{-1})	[C/Fe]	Selection	Notes
J122800.24-303137.6	50.4	...	...	...	...	...	v1	1, 2
J122851.02-300335.0	−91.8	...	...	...	...	...	v1	3
J122859.57-293619.2	7.7	...	...	...	...	...	v1	1, 2, 4
J122950.34-304017.2	85.1	4760	1.22	−2.41	2.20	...	v1	
J123015.17-305541.1	33.1	...	...	...	...	...	v1	1, 2
J123100.36-300953.2	57.1	...	...	...	...	...	v2	3
J123118.86-311401.9	48.4	...	...	...	...	...	v1	1
J123122.75-301530.1	75.5	4860	1.74	−2.21	1.50	...	v1	
J123221.73-285313.6	40.4	...	...	...	...	...	v1	1
J123227.40-301457.3	360.5	4682	1.07	−2.41	2.02	...	v1	

Notes. 1. Visual inspection revealed the target to be unambiguously metal-rich. 2. Ca II H and K in emission. 3. Broad spectral features. 4. Evidence of binarity.

(This table is available in its entirety in a machine-readable form in the online journal. A portion is shown here for guidance regarding its form and content.)

Table 3
Metal-poor Candidate Star Positions and Photometry

Object (2MASS)	RA	DEC	V	$B-V$	J	H	K	$W1$	$W2$
J121325.53-380021.6	12:13:25.5	−38:00:21	11.27	0.81	9.92	9.49	9.43	9.36	9.39
J121812.33-372106.5	12:18:12.3	−37:21:06	14.91	1.09	12.82	12.24	12.11	12.05	12.06
J122800.24-303137.6	12:28:00.2	−30:31:38	14.12	1.12	11.94	11.35	11.24	11.17	11.20
J122851.02-300335.0	12:28:51.0	−30:03:35	13.17	0.92	11.24	10.75	10.60	10.61	10.60
J122859.57-293619.2	12:28:59.6	−29:36:19	13.29	1.29	10.64	10.07	9.84	9.79	9.77
J122934.47-323307.4	12:29:34.4	−32:33:07	12.59	0.97	10.62	10.09	9.97	9.91	9.94
J122950.34-304017.2	12:29:50.3	−30:40:17	12.84	0.84	11.07	10.57	10.46	10.40	10.42
J123015.17-305541.1	12:30:15.2	−30:55:41	13.07	0.87	11.46	10.98	10.92	10.87	10.89
J123100.36-300953.2	12:31:00.4	−30:09:53	11.92	0.83	10.17	9.70	9.50	9.46	9.46
J123118.86-311401.9	12:31:18.9	−31:14:02	13.30	1.14	11.32	10.73	10.63	10.59	10.62

(This table is available in its entirety in a machine-readable form in the online journal. A portion is shown here for guidance regarding its form and content.)

equatorial coordinates made them easy to observe at low air mass from Las Campanas in June and July. We also focused on stars with $V \lesssim 13.5$.

4. DISCUSSION

We observed 239 stars selected using all seven criteria on our full APASS, 2MASS, and *WISE* data set. We designate these stars by "v2" in the selection column in Table 3. We identified four EMP stars with [Fe/H] $\lesssim -3.0$ and 73 very metal-poor (VMP) stars with $-3.0 \lesssim$ [Fe/H] $\lesssim -2.0$. In our candidate list, there were also five EMP stars and nine VMP stars that had already been discovered and that we would have observed had they been unknown. We list these stars in Table 4. We therefore estimate the efficiency of our selection as 9/253 for EMP stars and 82/253 for VMP stars, indicating fractional Bayesian selection efficiencies[11] of $3.8^{+1.3}_{-1.1}$% and $32.5^{+3.0}_{-2.9}$%. We observed 173 stars selected using criteria (1)–(5) on our pure infrared 2MASS and *WISE* data set. We designate these stars by "v1" in the selection column in Table 3. We identified 3 EMP stars and 35 VMP stars. We therefore estimate the efficiency of our selection as 3/173 for EMP stars and 35/173 for VMP stars, indicating fraction Bayesian selection efficiencies of $2.1^{+1.3}_{-1.0}$% and $20.5^{+3.2}_{-2.9}$%.

[11] See Section 3.3 of Schlaufman (2014) for a detailed discussion.

We plot in Figure 2 the posterior probability distribution for the fraction of carbon enhanced stars in our Magellan/MIKE sample of stars with [Fe/H] $\leqslant -2.5$. We use both the original definition of carbon enhancement [C/Fe] $> +1.0$ given in Beers & Christlieb (2005) and the update given in Aoki et al. (2007) accounting for stellar evolutionary effects

1. [C/Fe] $\geqslant +0.7$ for stars with $\log L/L_{\odot} \leqslant 2.3$,
2. [C/Fe] $\geqslant +3.0 - \log L/L_{\odot}$ for stars with $\log L/L_{\odot} > 2.3$.

Of our 29 stars with [Fe/H] $\leqslant -2.5$, none are carbon enhanced by the Beers & Christlieb (2005) definition, while 8 are carbon enhanced by the Aoki et al. (2007) definition. Carbon in the atmospheres of low surface gravity stars is mixed into the stellar interior, where it can be processed into nitrogen (e.g., Charbonnel 1995). The expected enhancement of nitrogen in the atmospheres of low surface gravity metal-poor stars has been observationally confirmed (e.g., Gratton et al. 2000; Spite et al. 2005). The dramatic difference in the carbon enhanced fraction between the two definitions emphasizes the importance of using the Aoki et al. (2007) definition to investigate carbon enhancement in stars above the horizontal branch.

We plot in Figure 3 the distribution of metal-poor stars from Yong et al. (2013a) with measured [C/Fe] in the log g–[C/Fe] plane. Evolved metal-poor stars like those in our sample typically have [C/Fe] $\lesssim +2.0$. We plot in Figure 4

Table 4
Previously Known Metal-poor Stars in Our Follow-up Target List

Object (2MASS)	Alias	$T_{\rm eff}$ (K)	log g	[Fe/H]	Reference
J121846.49-161050.8	HE 1216-1554	...	...	−3.33	Frebel et al. (2006b)
J123916.23-264746.8	...	...	...	−2.23	Harris (1996)
J123918.93-264941.9	...	...	...	−2.23	Harris (1996)
J125045.87-282656.3	...	...	...	−2.01	Morrison et al. (1990)
J131947.00-042310.2	HE 1317-0407	4525	0.30	−3.10	Hollek et al. (2011)
J143355.92-124035.7	HE 1431-1227	...	...	−2.58	Frebel et al. (2006b)
J212138.43-395612.9	BPS CS 30492-0116	...	...	−2.05	Beers et al. (2000)
J220216.36-053648.5	HE 2159-0551	...	...	−3.03	Frebel et al. (2006b)
J220841.10-394512.2	BPS CS 22881-0040	...	...	−2.27	Beers et al. (2000)
J221059.73-022525.2	HE 2208-0240	...	...	−2.06	Frebel et al. (2006b)
J222025.81-102320.2	BPS CS 22886-0042	...	...	−2.61	Aoki et al. (2007)
J230449.13-424348.0	HE 2302-4259	...	...	−3.15	Frebel et al. (2006b)
J231300.04-450706.6	HE 2310-4523	...	...	−2.60	Frebel et al. (2006b)
J232607.41-055006.9	BPS CS 22949-0048	4620	0.95	−3.37	Roederer et al. (2014)

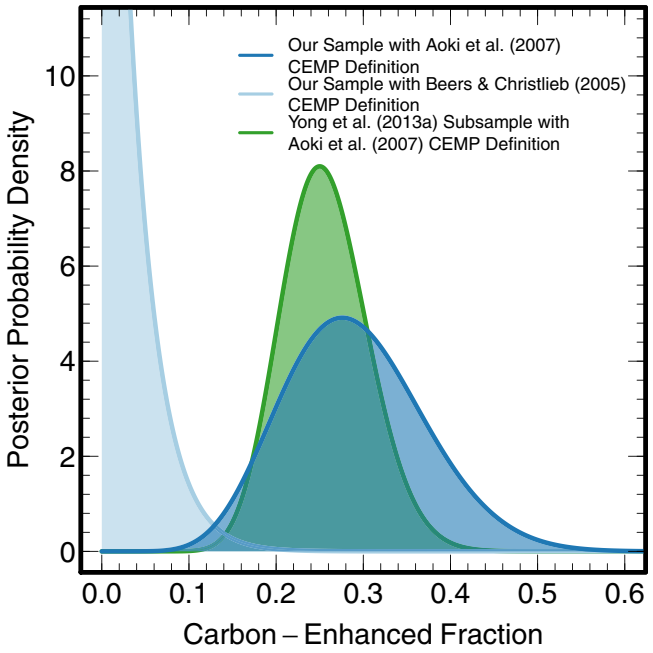

Figure 2. Posterior probability density of our carbon-enhanced fraction estimate. The dramatic difference for our sample between the Beers & Christlieb (2005) and the Aoki et al. (2007) definitions of carbon enhancement demonstrates the importance of the Aoki et al. (2007) definition's allowance for stellar evolution. The carbon-enhanced fraction in our sample of 29 stars with $-3.1 \leqslant$ [Fe/H] $\leqslant -2.5$ is fully consistent with the carbon-enhanced fraction in a subsample of stars with $-3.1 \leqslant$ [Fe/H] $\leqslant -2.5$ from Yong et al. (2013a).
(A color version of this figure is available in the online journal.)

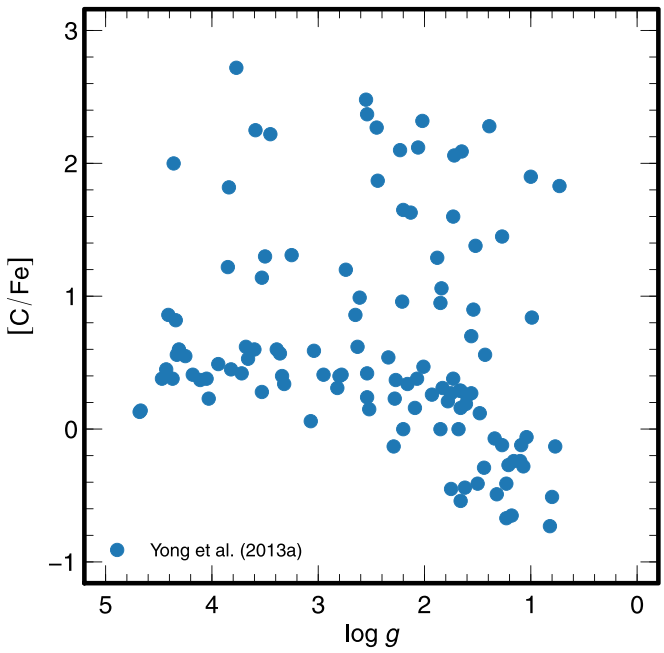

Figure 3. [C/Fe] vs. log g from Yong et al. (2013a). At log $g \approx 1.5$ typical of our sample, [C/Fe] $\lesssim 2.0$.
(A color version of this figure is available in the online journal.)

carbon-enhanced synthetic spectra from 1 to 6 microns. Our search efficiently selects stars with [Fe/H] ≈ -2.0 and [C/Fe] $\approx +0.0$. Since even a very carbon-enhanced EMP star with [Fe/H] ≈ -3.0 and [C/Fe] $\approx +2.0$ has weaker absorption in $W2$ than the aforementioned carbon-normal very metal-poor star, our search technique itself is not biased against carbon-enhanced EMP stars. While targeting carbon enhanced stars can increase the yield from EMP star searches, it can complicate the interpretation of the carbon-enhanced fraction. Conversely, further exploration using our selection will be able to provide an unbiased estimate of the carbon-enhanced fraction as a function of metallicity.

We plot in Figure 5 the apparent magnitude distribution of our metal-poor candidate population. There are 11,916 metal-poor candidates in our sample with $V < 14$. For comparison, at $V < 14$ there are 1800 HES candidates in the list of Christlieb et al. (2008), 1559 candidates in the list of Frebel et al. (2006b), and 125 HK candidates in the list of Beers et al. (1992). Given that $32.5^{+3.0}_{-2.9}$% of the targets chosen with our full selection have $-3.0 \lesssim$ [Fe/H] $\lesssim -2.0$ and $3.8^{+1.3}_{-1.1}$% have [Fe/H] $\lesssim -3.0$, in our sample one should be able to identify approximately 3900 VMP stars and 450 EMP stars with $V < 14$. APASS, 2MASS, and *WISE* data are available for the entire sky, so it will be possible for the first time to search for bright metal-poor stars in the entire northern sky as well as near the southern Galactic plane. Our candidate list is available upon request.

Of the giant stars targeted for moderate-resolution spectroscopy as part of HES follow up, about $40.0^{+1.2}_{-1.2}$% were found to have $-3.0 \lesssim$ [Fe/H] $\lesssim -2.0$ and $3.9^{+0.5}_{-0.5}$% were found to have [Fe/H] $\lesssim -3$ (e.g., Schörck et al. 2009). Combining its yield with the apparent magnitude distribution of its candidates, HES would be expected to find about 720 VMP giants

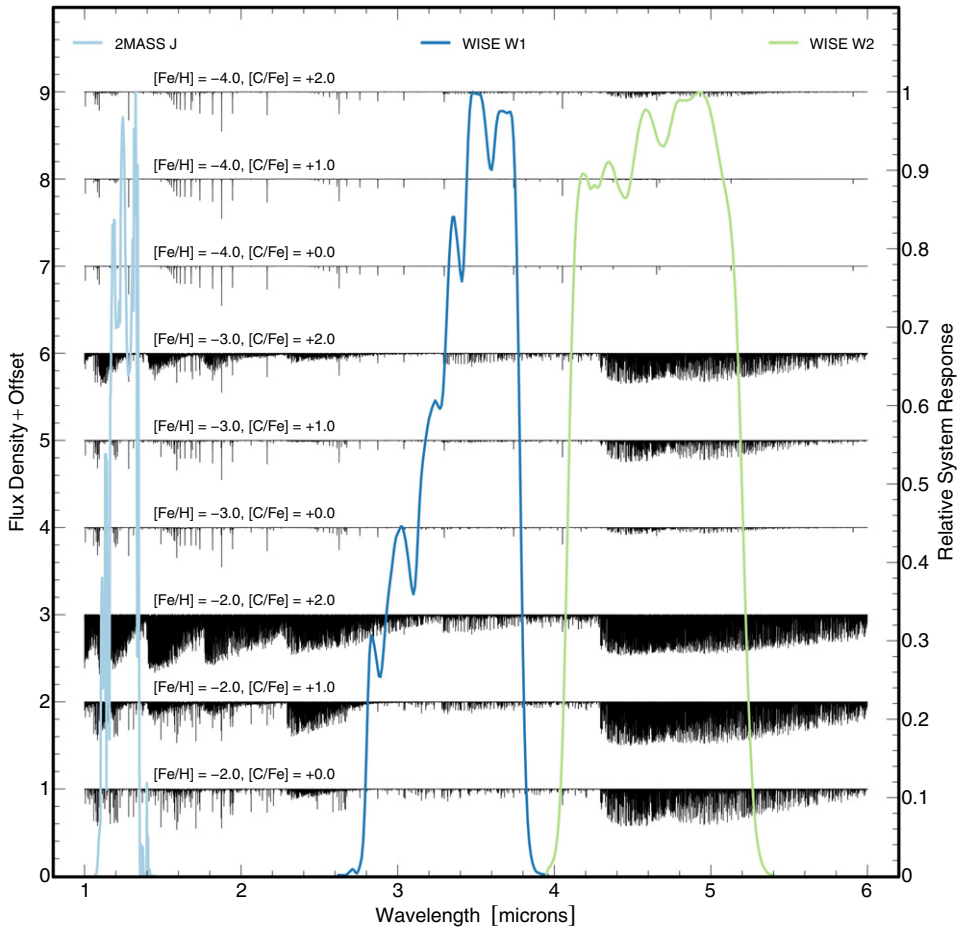

Figure 4. Theoretical spectra for stellar atmospheres with the metallicity and carbon enhancement given in the plot, assuming $[\alpha/\mathrm{Fe}] = +0.4$ (T. Masseron 2014, private communication). We assume $T_{\mathrm{eff}} = 4800$ K—the median of our sample—and $\log g = 1.5$, though the features are insensitive to $\log g$. The light blue curve is the RSR for the 2 MASS J band (1.2μ), the dark blue curve is the RSR for the *WISE* $W1$ band (3.4μ), and the green curve is the RSR for the *WISE* $W2$ band (4.6μ). Our selection correctly separates stars with $[\mathrm{Fe/H}] \approx -2.0$ and $[\mathrm{C/Fe}] \approx +0.0$ from the field population based on the weakness of molecular absorption in $W2$. An EMP star with $[\mathrm{C/Fe}] \approx +2.0$ still has weaker absorption in $W2$ than a star with $[\mathrm{Fe/H}] \approx -2.0$ and $[\mathrm{C/Fe}] \approx +0.0$, so our selection is unbiased against carbon-enhanced EMP stars. It is possible that our selection could miss stars with $[\mathrm{Fe/H}] \approx -2.0$ and $[\mathrm{C/Fe}] \gtrsim +0.0$.

(A color version of this figure is available in the online journal.)

and 70 EMP giants with $V < 14$. Of the apparently bright HES stars observed with moderate-resolution spectroscopy by Frebel et al. (2006b), about $8.7^{+0.7}_{-0.7}\%$ were found to have $-3.0 \lesssim [\mathrm{Fe/H}] \lesssim -2.0$ and $1.5^{+0.3}_{-0.3}\%$ were found to have $[\mathrm{Fe/H}] \lesssim -3$. Even though our selection efficiency is currently slightly less than HES, the larger number of candidates from our selection will allow a survey based on our selection to identify a larger number of apparently bright extremely metal-poor stars.

Our candidates are also bright in the sense that they are very luminous, among the most luminous known metal-poor stars. Using the scaling relation

$$L/L_{\odot} = (R/R_{\odot})^2 (T_{\mathrm{eff}}/T_{\mathrm{eff},\odot})^4, \quad (1)$$

$$= (M/M_{\odot})(g/g_{\odot})^{-1} (T_{\mathrm{eff}}/T_{\mathrm{eff},\odot})^4, \quad (2)$$

and taking the mass of our stars as $0.8 M_{\odot}$, the bolometric luminosity L of our stars can be approximated as

$$\log(L/L_{\odot}) = \log 0.8 - (\log g - 4.44) + 4 \log(T_{\mathrm{eff}}/5777\,\mathrm{K}). \quad (3)$$

We find that 24 of our stars with $[\mathrm{Fe/H}] \lesssim -2.0$ have $\log L/L_{\odot} \gtrsim 3$. That makes them more luminous than all of the metal-poor stars analyzed by Norris et al. (2013a, 2013b) and Yong et al. (2013a, 2013b) and comparable in brightness to the extremely distant and luminous stars identified by Bochanski et al. (2014a, 2014b) in the field and by several authors in dwarf spheroidal galaxies (Kirby et al. 2008; Frebel et al. 2010a, 2010b; Simon et al. 2010).

The bright absolute magnitudes of our metal-poor candidates suggests that at fainter apparent magnitudes, our selection can provide a large number of distant halo tracers. Distant halo tracers are important for kinematic estimates of the Milky Way's mass as well as the determination of the halo metallicity profile (e.g., Battaglia et al. 2005, 2006; Xue et al. 2008, 2014). We determine approximate distances for our Magellan/MIKE sample by interpolating a $[\mathrm{Fe/H}] = -2.5$, 10 Gyr Dartmouth isochrone (Dotter et al. 2008). We compute absolute $W1$ band magnitudes as a function of bolometric luminosity L from Equation (3), then derive the distance modulus for each of our metal-poor stars. At 100 kpc, one of our luminous metal-poor stars would have $V \approx 17.5$; near the Milky Way's virial radius at 200 kpc, one of our luminous candidates would have $V \approx 19$. To approximate the distance distribution of our entire sample, we convolve the apparent magnitude distribution of our entire candidate sample with the $W1$ absolute magnitude distribution of our Magellan/MIKE sample. We plot the result in Figure 6.

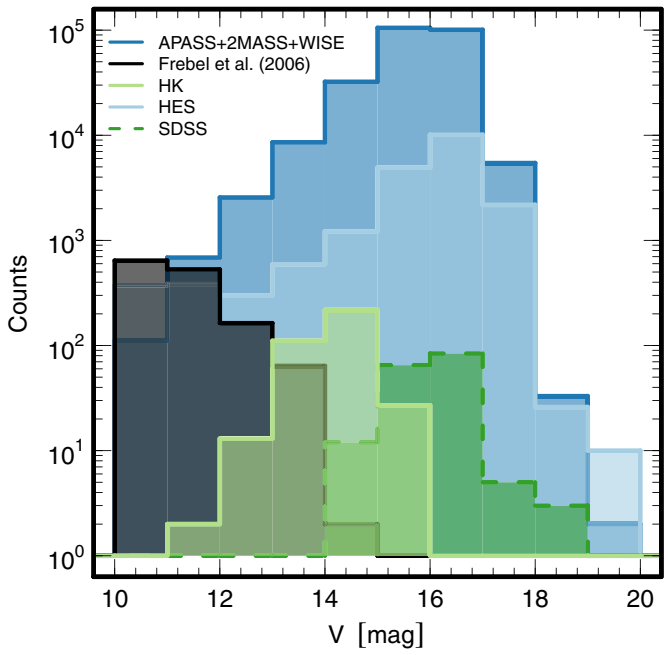

Figure 5. *V*-band magnitude distributions of candidate metal-poor stars. We plot the distributions from our selection (dark blue), the Frebel et al. (2006b) survey (black), the HK Survey (light green; Beers et al. 1992), and the Hamburg/ESO Survey (light blue; Christlieb et al. 2008). For EMP searches based on the SDSS, we plot the apparent magnitude distribution of confirmed EMP stars (dark green; Aoki et al. 2008, 2013; Bonifacio et al. 2012; Caffau et al. 2011b, 2012, 2013). That distribution is biased to bright apparent magnitudes compared to the candidate distribution, so the SDSS distribution should be understood as a bright limit to the SDSS metal-poor candidate distribution. For the SDSS sample, we have calculated approximate *V*-band magnitudes from the SDSS *gr* magnitudes using the metal-poor Population II color transformation of Jordi et al. (2006).

(A color version of this figure is available in the online journal.)

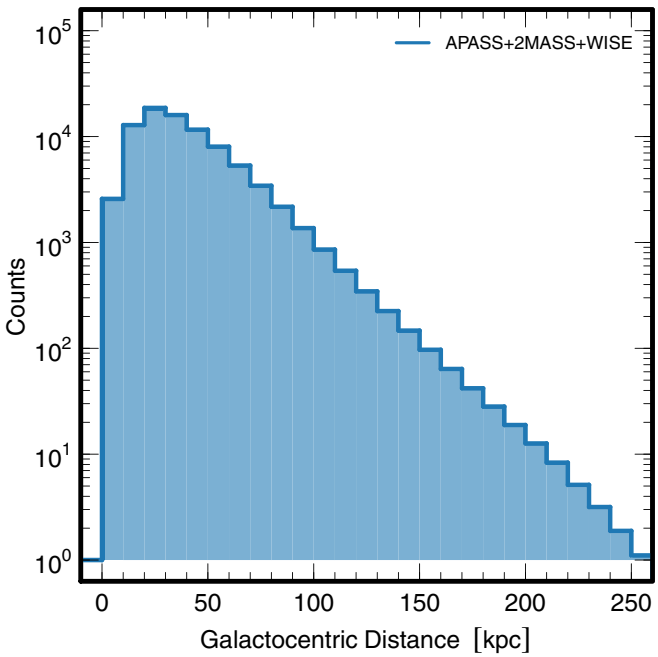

Figure 6. Distance distribution of our candidate metal-poor stars. The luminous nature of our candidates makes them excellent tracers of the distant halo.

(A color version of this figure is available in the online journal.)

Cooler stars are also more easily searched for signs of *r*-process enhancement than warmer stars, so our metal-poor giants are a better sample to constrain the *r*-process than a sample of warmer, metal-poor turnoff stars. Likewise, since cool stars typically have deeper lines at constant metallicity than warm stars, cool stars are the only way to learn about the detailed chemical compositions of the most metal-poor stars.

Should they persist, most of the Population III stars in the Galaxy are thought to currently reside in the bulge (e.g., Tumlinson 2010). Ground-based objective prism surveys are impractical in crowded bulge fields, while near UV based photometric searches like SkyMapper are effected by strong absolute and significant differential reddening. On the other hand, our photometric selection operates well even in crowded fields. Similarly, since the effects of extinction and reddening are ∼50 smaller in the *WISE* bands than in the optical (e.g., Yuan et al. 2013), our infrared selection is minimally effected by absolute or differential reddening. Indeed, if we take the distance to the Galactic Center as $R_0 = 8.2$ kpc (Bovy et al. 2009) and compute absolute $W1$ band magnitude as a function of L for our Magellan/MIKE sample, then two of our confirmed VMP stars are within about 2 kpc of the Galactic Center: 2MASS J181503.64-375120.7 and 2MASS J183713.28-314109.3. The former has [Fe/H] = −2.85 and the latter has [Fe/H] = −2.70. One of our confirmed EMP stars – 2MASS J155730.10−293922.7 – is approximately 4 kpc from the Galactic Center. These three stars are among the most metal-poor stars yet found in the bulge (Ness et al. 2013; García Pérez et al. 2013). Our selection can be extended to denser bulge fields with existing, high-resolution VISTA/VIRCAM VVV near-infrared and *Spitzer*/IRAC GLIMPSE mid-infrared data (Minniti et al. 2010; Saito et al. 2012; Benjamin et al. 2003; Churchwell et al. 2009). In the future, grism spectroscopy with NIRCam on the James Webb Space Telescope in bulge fields will be able to very efficiently select EMP stars based on the lack of molecular absorption in $R \sim 2000$ spectra between 2.4 and 5 μm (Rieke et al. 2005).

5. CONCLUSIONS

We have developed a metal-poor star selection that uses only public, all-sky APASS optical, 2MASS near-infrared, and *WISE* mid-infrared photometry to identify bright metal-poor stars through their lack of absorption near 4.6 microns. Our selection is efficient: our high-resolution follow-up observations confirmed that $3.8^{+1.3}_{-1.1}$% of our candidates have [Fe/H] $\lesssim -3.0$ and a further $32.5^{+3.0}_{-2.9}$% have $-3.0 \lesssim$ [Fe/H] $\lesssim -2.0$. We used our selection to identify seven previously unknown extremely metal-poor stars with [Fe/H] $\lesssim -3.0$ and a further 105 very metal-poor stars with $-3.0 \lesssim$ [Fe/H] $\lesssim -2.0$. In total, we identified 11,916 metal-poor star candidates with $V < 14$, increasing by more than a factor of five the number of publicly available metal-poor star candidates in this range of apparent magnitude. The bright apparent magnitudes of our candidates will enable a large survey based on our candidate list to significantly increase the number of extremely metal-poor stars with detailed chemical abundance measurements. Our infrared selection is well suited to the identification of metal-poor stars in the bulge, and two of our confirmed very metal-poor stars with [Fe/H] $\lesssim -2.7$ are within about 2 kpc of the Galactic Center. They are among the most metal-poor stars known in the bulge.

We thank Tim Beers, Anna Frebel, Jason Tumlinson, and Josh Winn. We are especially grateful to Thomas Masseron for providing unpublished carbon-enhanced synthetic spectra in the

infrared. This research has made use of NASA's Astrophysics Data System Bibliographic Services and both the SIMBAD database and VizieR catalog access tool, CDS, Strasbourg, France. The original description of the VizieR service was published by Ochsenbein et al. (2000). This research has made use of the NASA/IPAC Infrared Science Archive, which is operated by the Jet Propulsion Laboratory, California Institute of Technology, under contract with the National Aeronautics and Space Administration. This publication makes use of data products from the *Wide-field Infrared Survey Explorer*, which is a joint project of the University of California, Los Angeles, and the Jet Propulsion Laboratory/California Institute of Technology, funded by the National Aeronautics and Space Administration. This publication makes use of data products from the Two Micron All Sky Survey, which is a joint project of the University of Massachusetts and the Infrared Processing and Analysis Center/California Institute of Technology, funded by the National Aeronautics and Space Administration and the National Science Foundation. This research was made possible through the use of the AAVSO Photometric All-Sky Survey (APASS), funded by the Robert Martin Ayers Sciences Fund. This publication was partially based on observations obtained at the Gemini Observatory, which is operated by the Association of Universities for Research in Astronomy, Inc., under a cooperative agreement with the NSF on behalf of the Gemini partnership: the National Science Foundation (United States), the National Research Council (Canada), CONICYT (Chile), the Australian Research Council (Australia), Ministério da Ciência, Tecnologia e Inovação (Brazil) and Ministerio de Ciencia, Tecnología e Innovación Productiva (Argentina). A.R.C. acknowledges support through Australian Research Council Laureate Fellowship LF0992131, from the Australian Prime Minister's Endeavour Award fellowship for facilitating his research at MIT, and through European Research Council grant 320360: The *Gaia*-ESO Milky Way Survey. Support for this work was provided by the MIT Kavli Institute for Astrophysics and Space Research through a Kavli Postdoctoral Fellowship.

Facilities: CTIO:2MASS, FLWO:2MASS, Gemini:South (GMOS-S spectrograph), Magellan:Clay (MIKE spectrograph), Mayall (Echelle spectrograph), WISE

APPENDIX

DATA QUALITY FLAGS

We make four *WISE* data quality checks. First, that the *WISE* $W1$, $W2$, and $W3$ photometry be free of artifacts. Second, that the objects are fully consistent with a point source. Third, that the quality of the photometry in both $W1$ and $W2$ has been rated "A." Fourth, that the level of contamination by the Moon in $W1$, $W2$, and $W3$ be consistent with zero. The following SQL commands can be used to reproduce our initial selection by setting limits on an "All Sky Search" of the AllWISE Source catalog available from the NASA/IPAC Infrared Science Archive.[12]

```
j_m_2mass - h_m_2mass between 0.45 and 0.6
and w3mpro > 8
and w1mpro - w2mpro between -0.04 and 0.04
and j_m_2mass - w2mpro >= 0.5
and cc_flags like '000_'
and ext_flg = 0
and ph_qual like 'AA__'
and moon_lev like '000_'
```

[12] http://irsa.ipac.caltech.edu/Missions/wise.html

REFERENCES

Allende Prieto, C., Beers, T. C., Wilhelm, R., et al. 2006, ApJ, 636, 804
Aoki, W., Beers, T. C., Christlieb, N., et al. 2007, ApJ, 655, 492
Aoki, W., Beers, T. C., Lee, Y. S., et al. 2013, AJ, 145, 13
Aoki, W., Beers, T. C., Sivarani, T., et al. 2008, ApJ, 678, 1351
Aoki, W., Frebel, A., Christlieb, N., et al. 2006, ApJ, 639, 897
Battaglia, G., Helmi, A., Morrison, H., et al. 2005, MNRAS, 364, 433
Battaglia, G., Helmi, A., Morrison, H., et al. 2006, MNRAS, 370, 1055
Beers, T. C., Chiba, M., Yoshii, Y., et al. 2000, AJ, 119, 2866
Beers, T. C., & Christlieb, N. 2005, ARA&A, 43, 531
Beers, T. C., Preston, G. W., & Shectman, S. A. 1985, AJ, 90, 2089
Beers, T. C., Preston, G. W., & Shectman, S. A. 1992, AJ, 103, 1987
Benjamin, R. A., Churchwell, E., Babler, B. L., et al. 2003, PASP, 115, 953
Bernstein, R., Shectman, S. A., Gunnels, S. M., Mochnacki, S., & Athey, A. E. 2003, Proc. SPIE, 4841, 1694
Bochanski, J. J., Willman, B., Caldwell, N., et al. 2014a, ApJL, 790, L5
Bochanski, J. J., Willman, B., West, A. A., Strader, J., & Chomiuk, L. 2014b, AJ, 147, 76
Bonifacio, P., Sbordone, L., Caffau, E., et al. 2012, A&A, 542, A87
Bovy, J., Hogg, D. W., & Rix, H.-W. 2009, ApJ, 704, 1704
Brott, I., & Hauschildt, P. H. 2005, in The Three-Dimensional Universe with Gaia, Vol. 576, ed. C. Turon, K. S. O'Flaherty, & M. A. C. Perryman (Noordwijk: ESA), 565
Caffau, E., Bonifacio, P., François, P., et al. 2011a, Natur, 477, 67
Caffau, E., Bonifacio, P., François, P., et al. 2011b, A&A, 534, A4
Caffau, E., Bonifacio, P., François, P., et al. 2012, A&A, 542, A51
Caffau, E., Bonifacio, P., François, P., et al. 2013, A&A, 560, A15
Casey, A. R. 2014, arXiv:1405.5968
Castelli, F., & Kurucz, R. L. 2004, arXiv:astro-ph/0405087
Cayrel, R., Depagne, E., Spite, M., et al. 2004, A&A, 416, 1117
Charbonnel, C. 1995, ApJL, 453, L41
Christlieb, N., Schörck, T., Frebel, A., et al. 2008, A&A, 484, 721
Churchwell, E., Babler, B. L., Meade, M. R., et al. 2009, PASP, 121, 213
de Laverny, P., Recio-Blanco, A., Worley, C. C., & Plez, B. 2012, A&A, 544, A126
Dotter, A., Chaboyer, B., Jevremović, D., et al. 2008, ApJS, 178, 89
Foreman-Mackey, D., Hogg, D. W., Lang, D., & Goodman, J. 2013, PASP, 125, 306
Frebel, A., Aoki, W., Christlieb, N., et al. 2005, Natur, 434, 871
Frebel, A., Christlieb, N., Norris, J. E., Aoki, W., & Asplund, M. 2006a, ApJL, 638, L17
Frebel, A., Christlieb, N., Norris, J. E., et al. 2006b, ApJ, 652, 1585
Frebel, A., Kirby, E. N., & Simon, J. D. 2010a, Natur, 464, 72
Frebel, A., Simon, J. D., Geha, M., & Willman, B. 2010b, ApJ, 708, 560
Fulbright, J. P., Wyse, R. F. G., Ruchti, G. R., et al. 2010, ApJL, 724, L104
García Pérez, A. E., Cunha, K., Shetrone, M., et al. 2013, ApJL, 767, L9
Gratton, R. G., Sneden, C., Carretta, E., & Bragaglia, A. 2000, A&A, 354, 169
Harris, W. E. 1996, AJ, 112, 1487
Heger, A., & Woosley, S. E. 2010, ApJ, 724, 341
Henden, A. A., Levine, S. E., Terrell, D., Smith, T. C., & Welch, D. 2012, JAAVSO, 40, 430
Hollek, J. K., Frebel, A., Roederer, I. U., et al. 2011, ApJ, 742, 54
Hook, I. M., Jørgensen, I., Allington-Smith, J. R., et al. 2004, PASP, 116, 425
Irwin, J., & Bouvier, J. 2009, in IAU Symp. 258, The Ages of Stars, ed. E. E. Mamajek, D. R. Soderblom, & R. F. G. Wyse (Cambridge: Cambridge Univ. Press), 363
Jordi, K., Grebel, E. K., & Ammon, K. 2006, A&A, 460, 339
Keller, S. C., Bessell, M. S., Frebel, A., et al. 2014, Natur, 506, 463
Keller, S. C., Schmidt, B. P., Bessell, M. S., et al. 2007, PASA, 24, 1
Kirby, E. N., Simon, J. D., Geha, M., Guhathakurta, P., & Frebel, A. 2008, ApJL, 685, L43
Kordopatis, G., Gilmore, G., Wyse, R. F. G., et al. 2013, MNRAS, 436, 3231
Lee, Y. S., Beers, T. C., Masseron, T., et al. 2013, AJ, 146, 132
Mainzer, A., Bauer, J., Grav, T., et al. 2011, ApJ, 731, 53
Masseron, T., Plez, B., Van Eck, S., et al. 2014, arXiv:1410.4005
Merloni, A., Predehl, P., Becker, W., et al. 2012, arXiv:1209.3114
Minniti, D., Lucas, P. W., Emerson, J. P., et al. 2010, NewA, 15, 433
Morrison, H. L., Flynn, C., & Freeman, K. C. 1990, AJ, 100, 1191
Ness, M., Freeman, K., Athanassoula, E., et al. 2013, MNRAS, 432, 2092
Norris, J. E., Bessell, M. S., Yong, D., et al. 2013a, ApJ, 762, 25
Norris, J. E., Yong, D., Bessell, M. S., et al. 2013b, ApJ, 762, 28
Ochsenbein, F., Bauer, P., & Marcout, J. 2000, A&AS, 143, 23
Placco, V. M., Kennedy, C. R., Beers, T. C., et al. 2011, AJ, 142, 188
Placco, V. M., Kennedy, C. R., Rossi, S., et al. 2010, AJ, 139, 1051
Plavchan, P., Jura, M., & Lipscy, S. J. 2005, ApJ, 631, 1161
Reimers, D., & Wisotzki, L. 1997, Msngr, 88, 14

Rhee, J. H., Song, I., Zuckerman, B., & McElwain, M. 2007, ApJ, 660, 1556
Rieke, M. J., Kelly, D., & Horner, S. 2005, Proc. SPIE, 5904, 1
Roederer, I. U., Preston, G. W., Thompson, I. B., et al. 2014, AJ, 147, 136
Roederer, I. U., Sneden, C., Thompson, I. B., Preston, G. W., & Shectman, S. A. 2010, ApJ, 711, 573
Ryan, S. G., Norris, J. E., & Beers, T. C. 1999, ApJ, 523, 654
Saito, R. K., Minniti, D., Dias, B., et al. 2012, A&A, 544, A147
Schlaufman, K. C. 2014, ApJ, 790, 91
Schörck, T., Christlieb, N., Cohen, J. G., et al. 2009, A&A, 507, 817
Simon, J. D., Frebel, A., McWilliam, A., Kirby, E. N., & Thompson, I. B. 2010, ApJ, 716, 446
Skrutskie, M. F., Cutri, R. M., Stiening, R., et al. 2006, AJ, 131, 1163
Spite, M., Caffau, E., Bonifacio, P., et al. 2013, A&A, 552, A107
Spite, M., Cayrel, R., Plez, B., et al. 2005, A&A, 430, 655
Steinmetz, M., Zwitter, T., Siebert, A., et al. 2006, AJ, 132, 1645
Taylor, M. B. 2005, in ASP Conf. Ser. 347, Astronomical Data Analysis Software and Systems XIV, ed. P. Shopbell, M. Britton, & R. Ebert (San Francisco, CA: ASP), 29
Tumlinson, J. 2010, ApJ, 708, 1398
Wisotzki, L., Koehler, T., Groote, D., & Reimers, D. 1996, A&AS, 115, 227
Wright, E. L., Eisenhardt, P. R. M., Mainzer, A. K., et al. 2010, AJ, 140, 1868
Xue, X.-X., Ma, Z., Rix, H.-W., et al. 2014, ApJ, 784, 170
Xue, X. X., Rix, H. W., Zhao, G., et al. 2008, ApJ, 684, 1143
Yanny, B., Rockosi, C., Newberg, H. J., et al. 2009, AJ, 137, 4377
Yong, D., Norris, J. E., Bessell, M. S., et al. 2013a, ApJ, 762, 26
Yong, D., Norris, J. E., Bessell, M. S., et al. 2013b, ApJ, 762, 27
York, D. G., Adelman, J., Anderson, J. E., Jr., et al. 2000, AJ, 120, 1579
Yoshida, N., Omukai, K., Hernquist, L., & Abel, T. 2006, ApJ, 652, 6
Yuan, H. B., Liu, X. W., & Xiang, M. S. 2013, MNRAS, 430, 2188